Very high resolution satellite-based monitoring of crop (olive trees) evapotranspiration in precision agriculture

Nikolaos V. Spyropoulos*

Sigma Geotechnologie,
Rumfordstrasse 29, Munich, DE-80469, Germany
Email: nicospir@gmail.com
*Corresponding author

Nicolas R. Dalezios

Department of Planning and Regional Development,
University of Thessaly,
Pedion Areos, Volos GR-38334, Greece
Email: dalezios.n.r@gmail.com

Ioannis Kaltsis

Protypon SA,
Leoforos Vouliagmenis & Dodekanisou 3,
Alimos, GR-17456, Greece
Email: kaltsis@protypon.eu

Ioannis N. Faraslis

Department of Planning and Regional Development,
University of Thessaly,
Pedion Areos, Volos GR-38334, Greece
Email: faraslis@uth.gr

Abstract: Remote Sensing contributes through the processing and analysis of very high spatial and spectral resolution time series satellite data to a decision support at field level. In this paper, in the olive tree farms of the Agricultural Association of Messolonghi-Nafpaktia, the extraction of K_c and various vegetation indices, such as chlorophyll and red-edge, are presented aiming at the assessment of crop evapotranspiration and irrigation/fertiliser inflows during a period of 24 months. The methodology includes the generation of red-edge, chlorophyll and FPAR indices based on the second NIR band of WV-2, and clustering. The so-called $ET_{c(satellite)}$ produced by using the reference ET_o from FAO-56 Penman-Monteith equation, meteorological data set and $K_{c(satellite)}$ extracted by NDVI utilising the red-edge and second NIR bands of WV-2, respectively. The dynamic ET_d compared with ET_c. The applied methodology proved to be very useful for the implementation and verification of AGRO 2.1 and 2.2 standards.

Keywords: precision farming; remote sensing; WV-2; red-edge; chlorophyll index; normalised difference vegetation index; NDVI; Penman-Monteith; ET_c; K_c; AGRO.

Reference to this paper should be made as follows: Spyropoulos, N.V., Dalezios, N.R., Kaltsis, I. and Faraslis, I.N. (2020) 'Very high resolution satellite-based monitoring of crop (olive trees) evapotranspiration in precision agriculture', *Int. J. Sustainable Agricultural Management and Informatics*, Vol. 6, No. 1, pp.22–42.

Biographical notes: Nikolaos V. Spyropoulos is a geospatial intelligence evangelist with over 27 years of Earth observation (EO) and Satcom industry experience. His skills include exploitation of various EO missions and participation of several EU/ESA funded projects covering subjects such as environmental liability and security, geospatial intelligence and advanced information systems. He holds a PhD in Remote Sensing from Land Reclamation and Water Resource Management from the AUA University and MSc in Remote Sensing from UCL – Imperial College, London. He has been a Remote Sensing Lecturer at the AUA University and Joint Research Centre, Ispra.

Nicolas R. Dalezios is a Professor of Agrometeorology-Remote Sensing at the University of Thessaly (UTH), Greece. He is the Founding Director of the UTH Agrometeorology Laboratory, since 1991–2011. He obtained his Postgraduate in Meteorology (Athens, 1972) and in Hydrological Engineering (Delft, 1974) and PhD in Civil Engineering, University of Waterloo, Canada, in 1982. His research interests include agrometeorology, agrohydrology, remote sensing, environmental hazards, climate change and risk assessment. He is an author and/or co-author in over 400 refereed publications and technical reports. He is a reviewer and editorial board member in international scientific journals. He is an editor or co-editor in 15 edited publications, co-author in 30 book chapters, and author of two recent books (agrometeorology and environmental hazards).

Ioannis Kaltsis is an Agronomist graduate of the Agricultural University of Athens with an MSc in Food Industry Management and Marketing at Imperial College London and is the owner and CEO of Protypon SA. He is an expert consultant to organisations in the agri-food sector, responsible for the planning and development of agricultural management systems (Integrated Crop Management/AGRO 2, GLOBALGAP), food hygiene and safety management systems (ISO22000, BRC, IFS), environmental management systems (ISO 14001) and traceability systems of agricultural products in the food chain. He is also engaged in the development of GIS systems and electronic applications in agriculture especially in olive oil sector.

Ioannis N. Faraslis is a PhD researcher at the Department of Planning, Urban and Regional Development, University of Thessaly, Greece. Since 1999, he works at the Laboratory of Rural Space, Department of Planning, Urban and Regional Development of University of Thessaly in the fields of remote sensing and GIS sciences (image interpretation, aerial mapping using drones, classification analysis, change detection analysis, spatial modelling and DTM modelling).

1 Introduction

Olive groves and olive oil industry in Greece constitute a very important element for the Greek agricultural and food sectors. Greece is the third largest olive oil producer in the world with high percentage of the production to be of extra-virgin quality. The challenge for sustainable olive tree production is to achieve optimised yield (in quantity and quality) and farm income with a minimum of inputs (nutrients, water, energy, pesticides, herbicides, labour and money), while preserving and protecting the environment and social fabric.

For a long time, in satellite remote sensing, the emphasis was on geospatial vegetative analysis (Kanellou et al., 2011). It is gradually and steadily accepted that the red-edge spectral band can further contribute to the improvement of the accuracy and sensitivity of plant studies, despite the existing success of the normalised difference vegetation index (NDVI) method to measure plant features. The NDVI method is based on the principle that the chlorophyll in living plant material shows high absorption of the visible light and high reflection of the near-infrared light, thus, it is used to calculate and monitor vegetation. Moreover, WorldView-2 is a multispectral satellite, which provides very high resolution and global access to the red-edge spectral band, as well as two different infrared bands, one with less influence of the atmosphere. Similarly, satellites, such as Landsat-8, Spot-7, GeoEye-1 QuickBird and Ikonos, are multispectral providing two bands for routine calculation of the NDVI, i.e., a near-infrared band in the 750 nm to 890 nm range and a red band in the 610 nm to 680 nm range (Spyropoulos, 1999). Nevertheless, NDVI has been internationally effective in evaluating crop and forest health, monitoring environmental changes, as well as calculating plant vigour.

There is an increasing international interest to evaluate the red-edge region of the spectrum (between 680 nm and 750 nm), since hyperspectral sensors can measure numerous spectral bands. Indeed, the red-edge band is the transition region between the minimum and maximum reflectance. Specifically, the red-edge band can show differences between mature and young plants, can discriminate between species of weeds in crop fields, or can enhance the ability to segment between broad leafed plants and conifers.

Moreover, a comparison between red and red-edge bands can reveal differences between healthy trees and those affected by disease. Thus, a comparison between red and red-edge bands is more sensitive to detect changes in plant health than the NDVI. Research results indicate that far more sensitive and sophisticated analyses can be conducted by including the red-edge band. Based on extra red-edge and infrared channels, a new approach of K_c and ET_c monitoring may be considered. K_c is a variable crop coefficient that is changing though time due to the phenological cycle of a crop. K_c is also playing an enormous role in the fertilisation and irrigation process. K_c can be considered as analogous to vegetation indices, either derived by ground or satellite sensors (Dalezios et al., 2017).

RapidEye and Sentinel-2 A/B satellites with low to medium resolution (6–20 m) are still used to provide imagery that contains red-edge data and extra infrared data. These satellites can reveal insights into the conditions of a whole field, however, the current needs of segmentation necessary to assess large-scale details or the precision at farm level, such as the health of individual trees in very small orchard or map irrigation and fertilisation efficiency in a small field (Dalezios et al., 2014). The spatial and spectral resolutions of WV-2 imagery through the interrogation of the spectral bands can demonstrate variability of chlorophyll status and K_c at tree level (Yang et al., 2006).

The objective of this paper consists of assessing crop evapotranspiration (ET_c) and monitoring water needs in precision agriculture of olive trees. In the present study, derivatives, such as NDVI, crop coefficient (K_c), crop evapotranspiration (ET_c), chlorophyll, fraction of photosynthetically active radiation (FPAR), leaf area index (LAI), and soil-adjusted vegetation index (SAVI) (Colombo et al., 2003; Koch and Khosla, 2003) were produced. Clustering was used to identify variability in crop productivity potentially related to management practices, such as watering and fertilisation and to natural variations in soils. K_c and ET_c are derived from NDVI, using the red-edge and the second near-infrared band of WV-2, respectively. The geospatial analysis of the present study is structured on WorldView-2 optical sensor, which focuses on a specific range of the electromagnetic spectrum sensitive to a specific feature on the ground, or property of the atmosphere. The spectral bands are suitable to improve the segmentation and classification at the intra-olive trees or farm-paddock scale and satisfy the fragmentation characteristics of the southwestern Greek land-use. The paper is organised as follows: at first, the study area and the database are presented, followed be a thorough consideration of the methodology to estimate crop evapotranspiration in order to assess water needs in precision agriculture of olive trees based on very-high resolution satellite data (WV-2). Then, the results are presented and discussed.

2 Study area and database

2.1 Study area

The study area is in central western Greece and it is surrounded by the Acarnanian Mountains. The main river is the Acheloos River creating a rich fertile valley and an extensive wetland with rich biodiversity at its delta. Another smaller river is Evinos River located east of Messolonghi. Aitoliko and Messolonghi are the two lagoons found in the southern part of the region (Figure 1). The region is characterised by the lowest altitude in Greece, which is in west Aetolia-Acarnania and is about –10 metres below mean sea level. The area of interest (AoI) reduced to 100 sq-km with ground elevation ranging from 7 m in the south west flat areas to 492 m of small hills in the north east part of the area. The agriculture of the region is considered vulnerable due to increasing climate variability and change, which affects the water availability. The climatic conditions in the region range from hot and humid summers, with temperatures often surpassing 40°C, to mild and short winters in the low-lying areas, whereas in the mountain areas dominate cool winters. In the Panaitoliko Mountain, summers are cool and snow and cold weather dominate during winter months.

The Local Farmer's Association has a tradition of more than 80 years in the region. The Association was established in 1925 as Cooperative Paracheloitidas; in 1935, the Union of Agricultural Cooperatives of Messolonghi was created; in 1975, the area of Nafpaktias, called Union of Agricultural Messolonghi-Nafpaktias, was incorporated and finally Cooperatives in 2012 were converted into a primary cooperative under the name Agricultural Cooperative Messolonghi-Nafpaktias (The Union). The Union's scientific team includes high class agriculture engineers and agronomists with a vision to deploy the latest and greatest in the technological achievements to become a modern business unit with high quality amenities, in order to become a 'standard' cooperative emulated. Main activities are the harvesting, processing, standardisation of almost all agricultural commodities produced in the region, such as cotton, kalamata-type olives, Koutsourelis oil (from particular olive oil from the local Koutsourela variety), corn, grain and agricultural supplies market with ten stores. The cooperative operates from area Oiniades, Aggelokastro, Makrynia, Messolonghi Arakynthos, Evinochori, Makyneia, Nafpaktos and until recently Efpalio.

Figure 1 Location of the study area and specific location of the AoI (see online version for colours)

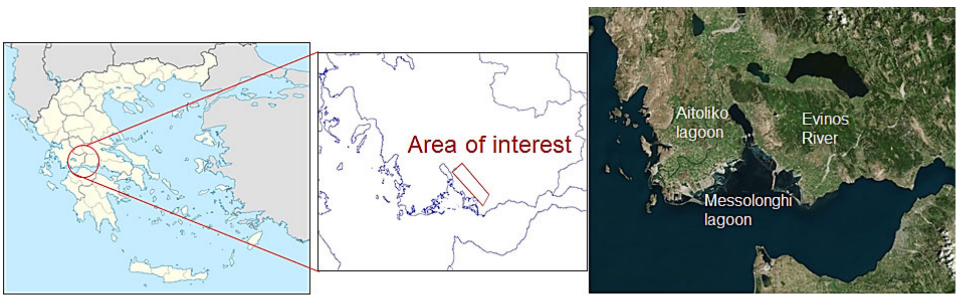

2.2 Database

In this study, satellite data were thoroughly considered. Ten WV-2 images of nine channels each (one pan + eight multispectral) were scheduled to be acquired during a period of 24 months. Each image was covering an area of 100 sq-km. The data acquired during winter and summer time, namely in Aug. 2013, Feb. 2014, July 2014, July 2014, Aug. 2014, Sep. 2014, March 2015, May 2015, June 2015 and July 2015, are in accordance with the farmer's calendar field activities that followed the Integrated Management AGRO 2.1 and 2.2 procedures for the olive trees in the region (Office for Official Publications of the European Communities, 2006). The total study area was 100 km^2 covering the budget of a minimum size of WV-2 image acquisition cost, and ten agricultural parcels well dispersed in the overall AoI selected and used to deploy the methodology. A 10 m digital elevation model (DEM) was built using 1/50,000 scale maps from the Hellenic Geographical Service of the Army for the entire area and 4 m DEM refined for each of the agricultural fields based on 1/5,000 scale topographic diagrams. Extensive field work to collect more than 120 ground control points (GCPs) was conducted during the early summer of 2013. Meteorological data (temperature, moisture, rainfall, wind, etc.) from the Aitoliko neighbouring meteorological station, which belongs to the National Observatory of Athens (NOA), were collected and analysed to generate the ET_o using the FAO-56 Penman-Monteith and the American Society of Civil Engineering (ASCE) Penman-Monteith equations, respectively. The geospatial analysis was based on Geomatica software package.

3 Methodology

The methodology is based on the hypothesis that it is possible to estimate seasonal water and nutrient needs of olive tree farms by cross correlating satellite data of high spatial, spectral and temporal resolution, which are acquired at well-defined time intervals of the phenological cycle of olive trees, having also simultaneous ground-truth information during the image acquisitions. This project demonstrates the coordinated efforts of remote sensing scientists, space engineers, satellite mission control planners, as well as teams of agronomists and environmentalists, to record the status of olive trees at specific time intervals of their phenological cycle from ground level and from 770 km above the Earth's surface, for subsequent cross-correlation and analysis. Satellite engineers and mission control planners tasked and programmed a specific orbit over a given areas in Greece and recorded a few minutes crop status also monitored by conventional methods by ground teams.

The degree of the difficultly of the project was very high. Flawless coordination by different professional teams was of paramount importance for successful execution of this project, and careful considerations of non-controlled parameters, such as weather, were considered. Weather conditions were the major non-controlled variable in the project (Dalezios et al., 2019, 2017; Stamatiadis et al., 2017). The whole project performed within an accuracy of less than 24 hours that included the execution of series of measurements by ground teams and the simultaneous satellite pass over the event area. It is obvious that the selection of the appropriate satellite orbit was guiding the execution of the ground team plans, which was not the case all the times due to operational and budgetary issues. More analytically, considerable effort deployed in the preparation, scheduling and acquisition of new satellite imagery, the satellite data management, the satellite data pre-processing and processing procedures including various NDVI indices, SAVI, LAI, FPAR and clustering (Dalezios et al., 2012). The basic principle that followed in the work is the estimation of $ET_{c(satellite)}$, which is based on the $K_{c(satellite)}$ derived from satellite data acquired during the crop season rather than FAO crop specific tables.

3.1 Step 1: spectral bands for vegetation behaviour

It is significant to understand the spectral bands and their relationship with plan behaviour. It is also very significant to understand the behaviour of vegetation in the wide range of the electromagnetic spectrum. It is also very significant to understand that the selection of satellite spectral bands is designed in such a way, that every time the energy emitted back to the sensor is measured either from the structure of the plan (growth indication or vigour) or the water content and pigments (senescence).

3.2 Step 2: building the vegetation knowledge in a geospatial intelligence environment at farm level

The vegetation knowledge in this paper is structured on WorldView-2 satellite image acquisitions, which is a commercial high-resolution satellite providing eight spectral sensors in the range between visible and near-infrared. Each sensor focuses on a specific range of the electromagnetic spectrum, which is sensitive to a specific feature on the ground, or a property of the atmosphere. These eight sensors are designed to improve the segmentation and classification of land and aquatic environments beyond any other space-based remote sensing platform.

The development of vegetation indices from satellite images have shown the potential to differentiate and map vegetation by providing valuable information about its structure and composition. In Mediterranean green areas, the NDVI, calculated by WV-2 having very high spatial resolution satellite data, has demonstrated that is an indicator of overall green biomass, tree density, canopy closure and tree species diversity, and thus, it seems a promising tool for analysing the vegetation of selected agricultural fields of the study area. The key point is that NDVI shows strong energy absorption by the chlorophyll in the red portion of the electromagnetic spectrum (RED), energy scatter by the internal structure of leaves in the near-infrared (NIR), and uses this contrast as an estimate of vegetation greenness, based on formula:

$$\text{NDVI} = (\text{NIR} - \text{RED}) / (\text{NIR} + \text{RED}) \tag{1}$$

Table 1 List of vegetation indices that can be used to build the crop intelligent information

Chlorophyll index	(NIR / GREEN) – 1 (*very useful for nitrogen fertilisation modelling*)
	(NIR / REDedge) – 1
Green NDVI	(NIR – GREEN / NIR + GREEN) (*index to extract senescence variations*)
Red-edge NDVI	(NIR – REDedge / NIR + REDedge) (*index to extract sensitive vegetation variations*)
Red-edge	RED / REDedge (*quick vegetation index*)
NIR/RED	NIR / RED (*quick vegetation index*)
NDVI	(NIR – RED) / (NIR + RED) (classic index to extract vegetation)
FPAR	FPAR = $c * [1 - a * \exp(-b * \text{LAI})]$ where a, b, c FPAR parameters (*index showing the chlorophyll behaviour*)
LAI	Leaf area index (*useful for vegetation modelling and satellite-based energy balance calculation*)
SAVI	Soil adjusted vegetation index (*especially used in a pre or early plantation phase*)

The result is an image with pixel values ranging theoretically from –1 to 1. In general, negative values correspond to non-vegetated surfaces, whereas positive values correspond to vegetated surfaces. Indeed, the lower NDVI values for vegetation usually start from 0.2–0.3. It should be mentioned that in areas with incomplete coverage by vegetation canopies, the NDVI is susceptible to spectral influence by the soil, leading to uncertainties in the interpretation. However, the impact of these uncertainties can also be the increase of the length of the NDVI gradient for certain vegetated surfaces, which could potentially improve the separation of land cover classes along this gradient. Table 1 list of vegetation indices that can be used to build the crop intelligent information.

In this paper, the vegetation knowledge is structured on the second NIR channel of the WV-2 satellite, which is less affected by the atmosphere, as well as on the red-edge and green channels.

3.3 Step 3: pan-sharpening and other indices (FPAR, SAVI, LAI)

3.3.1 The importance of pan-sharpening

Pan-sharpening is a digital synthesis, where the 2 m multispectral channels are merged with the 0.5 m panchromatic channel to generate another set of multispectral channels that preserve the spectral information, but in higher spatial feature space of 0.5 m, thus, enhancing the information integrity and clarity. Pan-sharpening is semi or fully automatic image fusion algorithm to increase the resolution of multispectral (colour) image data by using a high resolution black-and-white (panchromatic) image. The better the co-registration of the input panchromatic and multispectral (MS) image data is, the better the results from this function will be. If a geometric correction pre-processing step can improve this co-registration, then it should be considered. Atmospheric differences between the times at which the panchromatic and multispectral images are acquired will reduce the quality of the results from this function. Images that have been acquired simultaneously (WV-2) should be used, if possible. It is mentioned that the ratio of ground sample distances between the multispectral and panchromatic images should not exceed 5:1. For example, WV-2 data with 2 m MS and 0.5 m pan have a ratio of 4:1, which is acceptable. However, Landsat-8 30 m multispectral images have ~60 times the ground sample distance of WV-2 0.5 m panchromatic images, and an attempt to sharpen the former with the latter would produce poor results. Several image fusion algorithms have been tested, such as intensity hue and saturation (HIS). Typical problems found with existing algorithms include:

1 colour distortion

2 operator and dataset dependency.

Although the image fusion technique implemented in specific models, such as PANSHARP2 of PCI Geomatics (developed by Dr. Yun Zhang, Department of Geodesy and Geomatics Engineering, University of New Brunswick), diminishes greatly those deficiencies, no algorithm is known to produce ‘perfect’ results (Xu et al., 2014).

The pan-sharpened multispectral images are expected to inherit the level of spatial information from the panchromatic image data, but it is not expected to benefit from colour information to guarantee ‘true’ high resolution multispectral images. Thus, spatial features of sizes smaller than the multispectral sensor resolution may be assigned ‘fake’ colour, although visually the image quality appears to be excellent. The PANSHARP2 algorithm of the company PCI Geomatics produces best results for multispectral image channels, whose wavelengths lie within the frequency range of the panchromatic image channel. Moreover, multispectral channels outside the wavelength range of the high-resolution panchromatic image channel will still look good, although their physical meaning may have been reduced.

3.3.2 Other indices (SAVI, LAI, FPAR)

The SAVI, LAI and FPAR algorithms are also used, which are included as given routines in most of the remote sensing software packages. The indices and the ready-made routines are applied onto 2 m multispectral data and on pan-sharpened 0.5 m data.

SAVI is an index based on the red and near-infrared bands to measure the density and vigour of green vegetation by eliminating the reflectivity of the ground beneath the canopy (Huete, 1988). SAVI requires first the data to be atmospherically corrected. SAVI is calculated using the following equation:

$$\text{SAVI} = a_0 - a_1 * \exp\left(-a_2 * \text{LAI}\right) \tag{2}$$

where a_0, a_1 and a_2 are three parameters which can be specified by the user. The default values that were used are: $a_0 = 0.75$, $a_1 = 0.65$ and $a_2 = 0.6$, respectively.

The LAI is an index, which refers to the density of the green leaves in an area and measures the green leaf area (one-side) per unit of surface area. LAI can only approximate typical trends in vegetation. It is not advisable to be used for replacing or confirming field measurements of other types of vegetation in different seasons. LAI on NDVI is based on the visible and near-infrared bands to measure the density and vigour of green vegetation by comparing the amount of visible light reflected with the amount of near-infrared light reflected (Bannari et al., 2002). The defaults provided for equations are typical for wheat. By using a constant set of values, either custom or default, to calculate the LAI for images of the same area over time, it is possible to uncover trends in the vegetation. LAI calculates the leaf area index model channel. To run LAI, it must first run the atmospheric correction for RED and NIR sensor band channels (ATCOR2 or ATCOR3). LAI is calculated using the following equation:

$$\text{NDVI} = a_0 - a_1 * \exp\left(-a_2 * \text{LAI}\right) \tag{3}$$

where a_0, a_1 and a_2 are three parameters, which are specified above. Remote sensing provides a method to obtain repeated, rapid and inexpensive estimates of the fraction of absorbed photosynthetically active radiation (FAPAR) over large areas, whereas ground-based FPAR measurements are time consuming and labour intensive. The FPAR is a key parameter for ecosystem modelling, crop growth monitoring and yield prediction. The FPAR equation normally uses the red and near-infrared bands to calculate the fraction of radiation between 400 and 700 nm absorbed by green vegetation. The FPAR equation contains three parameters, whose values depend on the type of vegetation being measured and on the season in which they are being measured (Asrar et al., 1984; Wiegand et al., 1992). The equation also includes the result from the LAI. By using a constant set of values, either custom or default, to calculate the FPAR for images of the same area over time, the user can uncover trends in the vegetation. To run FPAR, RED and NIR channels must be atmospherically corrected using either ATCOR2 or ATCOR3 programs. FPAR is calculated using the following equation:

$$\text{FPAR} = c * \left[1 - a * \exp(-b * \text{LAI})\right] \tag{4}$$

where a, b and c represent parameters specified by the user. The default values for a, b and c are: $a = 1.0$, $b = 0.4$ and $c = 1.0$, respectively. The maximum value for any of the three parameters is 10.0.

3.4 Step 4: estimating the FAO-56 ET_o

First, the following FAO-56 Penman-Monteith equation was used to estimate the reference ET_o

$$ET_o = \frac{0.408\Delta(R_n - G) + \gamma \frac{900}{T+273} u_2 (e_s - e_a)}{\Delta + \gamma(1 + 0.34u_2)} \tag{5}$$

where

ET_o reference evapotranspiration (mm day^{-1})

R_n net radiation at the crop surface (MJ m^{-2} day^{-1})

G soil heat flux density (MJ m^{-2} day^{-1})

T mean daily ait temperature at 2 m height (°C)

u_2 wind speed at 2 m height (m s^{-1})

e_s saturation vapour pressure (kPa)

e_a actual vapour pressure (kPa)

$e_s - e_a$ saturation vapour pressure deficit (kPa)

Δ slope vapour pressure curve (kPa $°\text{C}^{-1}$)

γ psychrometric constant (kPa $°\text{C}^{-1}$).

Secondly, the ASCE Penman-Monteith equation was also used to generate the ET_o

$$ET_o = \left(\frac{\Delta(R_n - G) + K_{time}\rho_a c_p \frac{(e_s - e_a)}{r_a}}{\Delta + \gamma\left(1 + \frac{r_s}{r_a}\right)} \right) \Big/ \lambda \tag{6}$$

where

ET_o reference evapotranspiration (mm day^{-1})

R_n net radiation calculate using FAO-56 procedures (Allen et al., 1998)

ρ_a mean air density at constant pressure (kg m^{-3})

c_p specific heat of the air (MJ kg^{-1} $°\text{C}^{-1}$)

r_s bulk surface resistance (37 s m^{-1}) based on L5 thermal band data

r_a aerodynamic resistance (320 s m^{-1}) based on L5 thermal band data

$e_s - e_a$ saturation vapour pressure deficit (kPa)

λ latent heat of vaporisation (MJ kg^{-1})

K_{time} unit conversion (86,400 s d^{-1} for ETO in mm d^{-1} and 3,600 s h^{-1} for ET in mm h^{-1}).

3.5 Step 5: estimating the irrigation water needs by calculating the crop ET from satellite data

According to this methodological process, it is possible to estimate the irrigation water needs of a crop by calculating the *ET* from satellite data by mainly using the K_c coefficient, which is also derived through the previously described vegetation knowledge, such as vegetation index (VI).

Calera et al. (2017) estimated the water irrigation needs of a crop by calculating the *ET* from satellite data by mainly using the K_c coefficient, which is derived by a VI. The full *ET* estimation equation is based on:

$$ET = \left(K_s * K_{cb} + K_e\right) ET_o \quad (7)$$

The basal crop coefficient (K_{cb}) is defined as the ratio of the crop evapotranspiration over the reference evapotranspiration (ET_c / ET_o) for a dry soil surface, however, transpiration is occurring at a potential rate, i.e., water is not limiting transpiration. As a result, the term K_{cb} ET_o represents primarily the maximum transpiration component of ET_c of an unstressed canopy. The K_{cb} ET_o includes a residual diffusive evaporation component supplied by soil water below the dry surface (K_e) and water stress coefficient K_c, which refers to the soil water from the beneath dense vegetation. Moreover, the term K_s K_{cb} ET_o represents the actual transpiration of a canopy and the term K_e ET_o is the evaporation from bare soil fraction. The term K_c is a spectral crop coefficient that takes values between 0.15 and 1.20. Dercas et al. (2017) have used the following equation based on WV-2 data over wheat and corn farms in central Greece.

$$K_c = 1.33 * \text{redNDVI} + 0.21 \quad (8)$$

In this present paper, K_c is calculated from a red NDVI, which is a modified version of the following equation built in Pleiades, a European Union funded project.

$$K_c = 1.15 * \text{NDVI} + 0.17 \quad (9)$$

However, it should be mentioned that the above K_c coefficients are based on Landsat-5 Thematic Mapper spectral bands, which have different bandwidth in green, red and near-infrared wavelengths from WV-2, which also includes a red-edge channel.

4 Results and discussion

WV-2 proved to be very interesting for small-scale olive tree farms and for the extraction of bio-geophysical parameters. The selection of WV-2 data was based on:

1. Their spectral bands availability is supporting mainly the red-edge band and the second near-infrared band that has less influence by the atmosphere.
2. Spatial resolution of 0.5 m in pan band and 2 m in multispectral bands, but 0.5 m in the pan-sharpened mode.
3. Precision and information accuracy (< 2 metres) with GCPs to create actionable intelligence for the farmers.

There is a gradual tendency for location-based systems, leading to the need for high accuracy and precision to ensure that imagery and derived information can be used for actionable intelligence for a variety of applications, such as agriculture, including precision farming. Specifically, imagery's positional accuracy has been steadily improving from error margins around 23 metres in the early 2000s to less than 3 metres today. Increased accuracy is primarily due to more stable satellite orbits and innovative post-processing techniques that reduce error margins. There are several technologies that enable efficient registration of data to a base map, showing both imagery and vector base layers. This practice is referred to as 'second generation ortho', where a new image is registered to a base map that is, in turn, used for maintenance and updates of geospatial databases aligned to the base map. The geolocation accuracy with WV-2 was better than 1 m using GCPs and DEM (pan-sharpened data) instead of 10 m of Sentinels, thus provided more correlation of the what-you-see-is-what-you-get (WYSIWYG).

Figure 2 Comparison of calibrated FPAR from fertilisation to full growth month (see online version for colours)

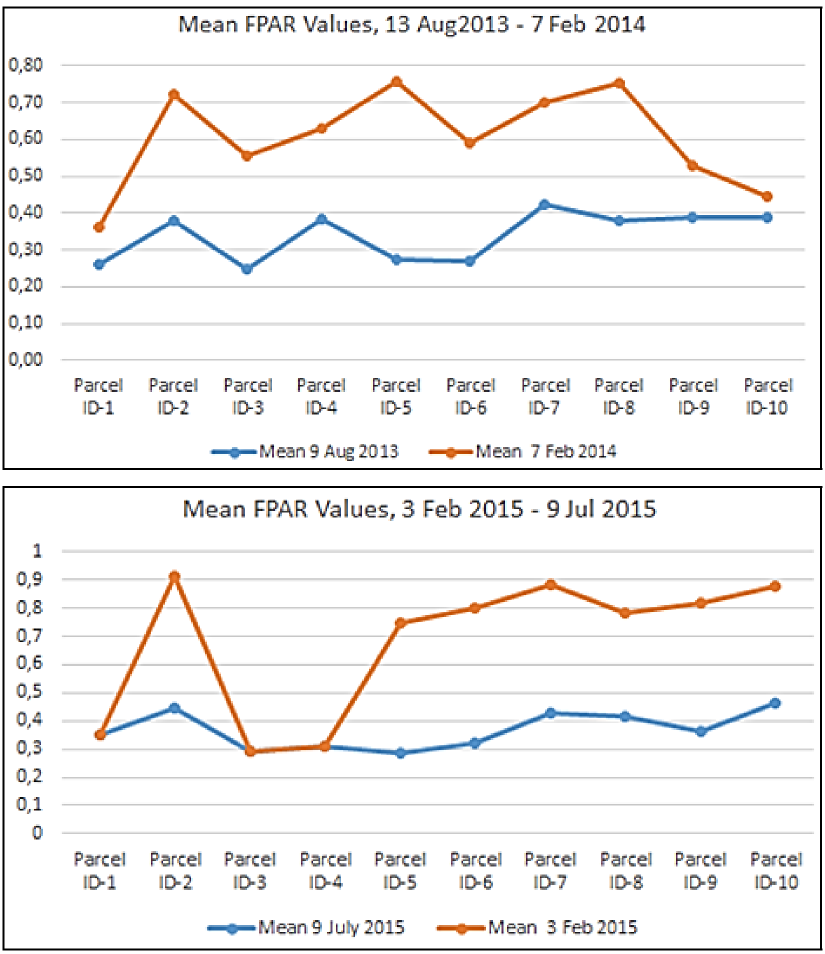

Note: Zero values mean that the specific parcel was either under cloud or cloud shadow coverage during the satellite pass.

For each agricultural parcel, the corresponding WV-2 images were atmospherically and radiometrically corrected (Updike and Comp, 2010) and then based on calibrated data several indices were developed, such as:

- chlorophyll index
- green NDVI
- red-edge NDVI
- red-edge
- NIR/RED
- NDVI
- FPAR.

The indices were applied onto 2 m multispectral data and on pan-sharpened 0.5 m data. The results show that the behaviour of the vegetation indices is the same irrespective of multispectral or pan-sharpened data used in the generation of vegetation knowledge. However, the pan-sharpened bitmaps exhibit a better clarity and assist in the understanding by a non-experienced user, as they represent the real world with better accuracy and integrity in terms of information content. This allows also a more accurate scouting or field work by farmer or teams to selected subareas or zone polygons that exhibit anomaly in spectral patterns. The NDVI and red-edge NDVI indices from multispectral and pan-sharpened data are used to cross correlate evapotranspiration, K_c, chlorophyll status with crop water and nutrition needs provided by the farmers (their AGRO calendars). The NDVI that was based on red-edge and second NIR bands exhibited interesting visual results (less atmospheric absorption).

Table 2 Mean FPAR values distribution for each agricultural parcel: summer 2013–winter 2014 and winter 2015–summer 2015

	FPAR VALUES			
	13-Aug-2013	*7-Feb-2014*	*3-Feb-2015*	*9-Jul-2015*
Parcel ID	Mean	Mean	Mean	Mean
1	0.26	0.36	0	0.35
2	0.38	0.72	0.47	0.44
3	0.25	0.56	0	0.29
4	0.38	0.63	0	0.30
5	0.28	0.76	0.46	0.28
6	0.27	0.59	0.47	0.32
7	0.42	0.70	0.45	0.43
8	0.38	0.75	0.37	0.41
9	0.39	0.53	0.45	0.36
10	0.39	0.45	0.42	0.46

The FPAR results were very interesting and were used to understand the chlorophyll status, which was also an indicator of N uptake. Even for the small and fragmented parcels in the AoI, the WV-2 data provided an alternative and unique method to obtain repeated, rapid and inexpensive estimates of FPAR. These passive remote sensing data have been used to derive FPAR using radiative transfer models or empirical relationships between FPAR and vegetation indices. This relationship is linear or close to linear between VI and FPAR (Fensholt et al., 2004). In our FPAR case, red-edge and the second near-infrared channel was used. From Table 2 and Figure 2, it can be stated that in February, which is normally the fertilisation month for olive trees, the FPAR exhibits higher mean values than summer months.

Figure 3 (a) The 2014 $K_{c(satellite)}$ generated from the monitored agricultural parcels (5 to 10) in the AoI* (b) The 2014 $ET_{c(satellite)}$ generated from the monitored agricultural parcels (5 to 10) in the AoI** (see online version for colours)

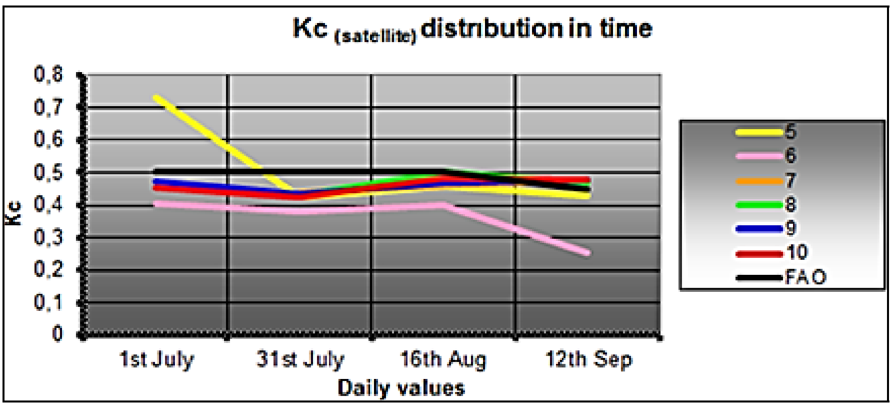

(a)

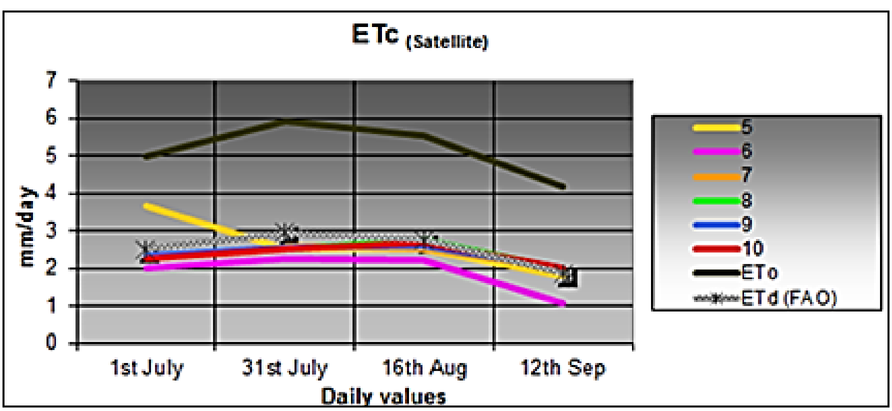

(b)

Notes: *The FAO reference K_c is drawn with black line.
**The reference ET_o and ET_d from FAO tables is drawn with black solid and dashed lines.

For each farm plot, diachronic indices are created to build a satellite-based farm profile, which is compared to farmer AGRO standard agricultural practices. K-means clustering is used to produce precision farming spatio-temporal thematic maps. Six well-identifiable classes are selected, such as olive trees, soil type A, soil type B, bare soil, shadows and artificial surfaces. The diachronic maps are overlaid then onto corresponding pan-sharpened false colour composite (red-edge, green and blue channels) for viewing purposes. This process shows the dramatic land-use change nearby the olive groves. Especially for mature olive groves in the study area farms, the within farm $K_{c(satellite)}$ variability can be extracted and it is very likely to be able to monitor the individual tree behaviour in conjunction with the farmer agricultural practices and local climate. The ET_o generated from equations (5) and (6) produces very similar values, with the ASCE to be slightly lower from the classic FAO-56 model by second decimal digit. In the subsequent processing, the FAO-56 reference ET_o is decided to be used (Yoder et al., 2005). The K_c from FAO had a very 'flat' behaviour, meaning that the values were 0.45 in June to 0.50 in July and August and back to 0.45 in September (Papazafeiriou, 1999). The $K_{c(satellite)}$ is derived from equation (9) and it is used to generate the $ET_{c(satellite)}$. Figures 3(a) and 4(a) show the chronological distribution of $K_{c(satellite)}$ from all parcels under study along with the K_c from FAO, just for comparison.

Figure 4 (a) The 2015 daily $K_{c(satellite)}$ generated from the monitored agricultural parcels (2 to 10) in the AoI* (b) The 2015 daily $ET_{c(satellite)}$ generated from the monitored agricultural parcels (2 to 10) in the AoI** (see online version for colours)

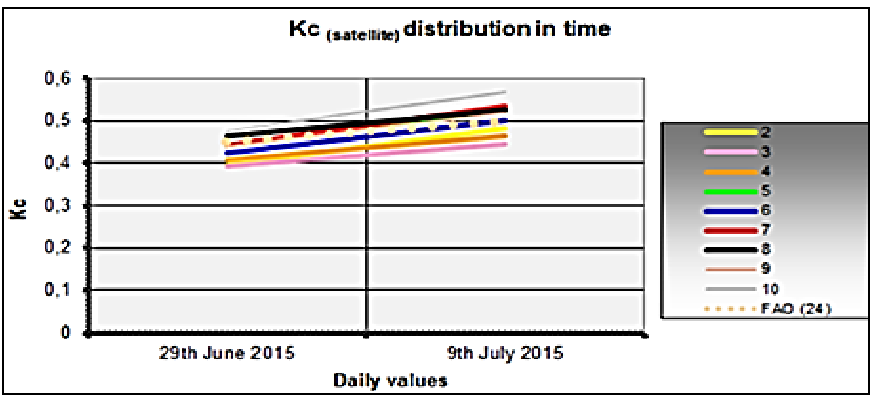

(a)

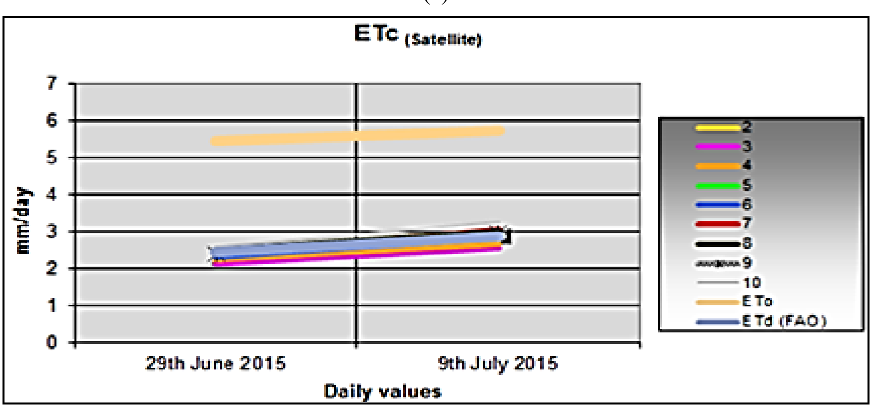

(b)

Notes: *The FAO reference K_c is drawn with dotted grey line respectively.
**The reference ET_o and ET_d from FAO tables is drawn with grey solid and cyan lines, respectively.

Then, the $ET_{c(satellite)}$ is calculated using the following equation:

$$ET_{c(satellite)} = K_{c(satellite)} * ET_o \tag{10}$$

Also, Figures 3(b) and 4(b) show the results for the calculation of the reference ET_o, ET_c from FAO-56 Penman-Monteith and from $ET_{c(satellite)}$, respectively. The $ET_{c(satellite)}$ is following the general pattern of the dynamic ET_d curve, but it is more adapted to the phenological cycle of the crop and local climatic conditions. Table 3 summarises the $K_{c(satellite)}$, $ET_{c(satellite)}$ derived by WV-2 and K_c, ET_o and ET_d derived by FAO. Corresponding months are June 2015 and July of 2015.

Table 3 June and July of 2015, $K_{c(satellite)}$ and $ET_{c(satellite)}$ compared to K_c, ET_o and ET_d from FAO

	*$K_{c(satellite)}$ = [1, 15 * RedEdgeNDVI+0, 17]*		*$ET_{c(satellite)}$*	
	Months		*Months*	
Parcel ID	*29th June 2015*	*9th July 2015*	*29th June 2015*	*9th July 2015*
1	[redacted]			
2	0.395	0.483	2.14485	2.763726
3	0.393	0.444	2.13399	2.540568
4	0.409	0.465	2.22087	2.66073
5	0.443	0.525	2.40549	3.00405
6	0.425	0.499	2.30775	2.855278
7	0.442	0.533	2.40006	3.049826
8	0.464	0.526	2.51952	3.009772
9	0.439	0.518	2.38377	2.963996
10	0.477	0.569	2.59011	3.255818
K_c FAO (24)	0.45	0.50	[redacted]	
ET_o	[redacted]		5.43	5.722
ET_d (FAO)	[redacted]		2.4435	2.861

The spatial distribution of $ET_{c(satellite)}$ during summer months of 2013, 2014 and 2015 in relation of the Aitoliko meteorological station also mapped. Aitoliko station belongs to the meteor network of NOA and it is located in the Aitoliko lagoon coastline, (lat.: 38.43597°N, long.: 21.36363°E, altitude: 3 m). The station facility is also less than 10 km distance from the agricultural farms in the study area. Six major $ET_{c(satellite)}$ spatial zones have been depicted ranging from less than 2.5 mm/day to more than 7 mm/day corresponding to the local topography with small hills in north east and south west and valley in between, drainage network with a flow direction from north east to south west and mixed and multiple vegetation types. The olive tree farms under study have representatives in most of the zones (Figure 5).

Figure 5 $ET_{c(satellite)}$ spatially distributed zones overlaid onto the WV-2 image (grey polygon) (see online version for colours)

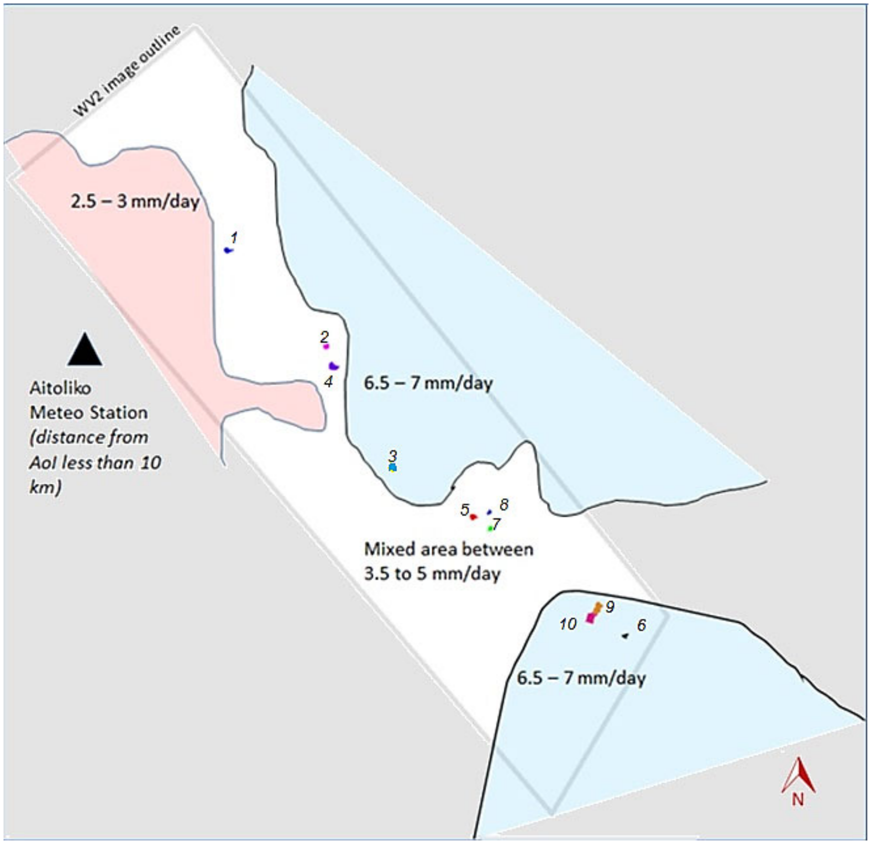

Notes: Three zones: cyan, light brown and white. A 'virtual valley' of lower values is created, coinciding with the topography of the area. High $ET_{c(satellite)}$ values are observed in the north east/south west parts of the image and lower values in central/north west part. Small numbered polygons are the IDs of the studied parcels, which are dispersed in the study area. Aitoliko meteorological station is less than 10 km from the farms.

By extracting the $ET_{c(satellite)}$ to the area of per sq-m in each parcel, it was possible to estimate the evapotranspiration water requirements from this specific parcel against irrigation needs. Comparing the water requirements from FAO-56 and from WV-2 data, it was likely to see the differences in water quantities for 29th June 2015 and 9th July 2015. For both months, the overall requirements estimated by satellite data were less than the needs estimated by FAO (8 m^3 less for June 2015 and 2 m^3 less for July 2015, respectively) and this is mainly due to the dynamic character of satellite data, which reflect the phenological cycle of the crop, the weather and the applied agricultural practices of the farmer (Table 4). The Agricultural Association of Messolonghi-Nafpaktia counts of 930 members with an overall irrigated area of 2,552.2 hectares (ha). In 29th of June 2015 and 9th July 2015, the irrigated water consumption was 450,000 cm and 518,000 cm, respectively, using drip irrigation. Projecting those numbers to mean irrigation dose for the whole irrigated area, the farmers applied 176 m^3/ha and 203 m^3/ha for 29th of June 2015 and 9th July 2015, respectively. The mean evapotranspiration from the 7.4 hectares of the pilot-farms area on the specific day of the satellite pass was 23 m^3/ha for 29 June 2015 and 29 m^3/ha for 9 July 2015, respectively. From FAO tables, the corresponding potential evapotranspiration was 24 m^3/ha and 29 m^3/ha for 29 June 2015 and 9 July 2015, respectively, but these numbers are calculated with a fixed K_c for the whole duration of each month. The one cubic metre less water requirements difference in 2,552 hectares in June 29th is 2,552 m^3 less water for the whole area of the farmers' association, which could be saved from the monthly irrigation scheme and cost. For example, having a mean cost of 0.20 €/m^3 for the irrigation water, it can be stated that the cost of water saving in June 29th 2015 is 510 €/m^3, and if this difference is maintained for the whole critical months of olive groves for March, April, May, June, July and Aug., then the cost saving could reach approximately the amount of 50,000 €/m^3 per growing season, by considering that the above numbers are based on specific days. Regarding the cost of WV data procurement, according to Maxar satellite operator, a single scene of 100 sq-km can be purchased at 17 euro/sq-km. Then, a ten-day time series data will generate a cost of 5,100 euro per month or 30,600 euro in six-month period. This cost is still considerable, which means that the satellite data should not be used in a fragmentary manner for very small agricultural areas, which are covering a small part of the image, but in a well-defined regional or even national plan, where most of the agricultural parcels or AoI will ideally match the image collection scenario.

Table 4 Summer 2015 monthly water requirements for each monitored agricultural parcel

Parcel ID	*Square meters*	*ET_c(sat) June 29th 2015*	*ET_c(sat) July 9th 2015*	*Specific day water needs (m^3), June 29th 2015*	*Specific day water needs (m^3), July 9th 2015*	*FAO June water needs (m^3)*	*FAO July water needs (m^3)*
1	[redacted]						
2	2,824	2.41	3.00	6.79	8.48	6.99	8.36
3	2,364	2.22	2.66	5.25	6.29	5.85	7.00
4	12,668	2.13	2.54	27.03	32.18	31.35	37.50
5	2,768	2.14	2.76	5.94	7.65	6.85	8.19
7	2,776	2.40	3.05	6.66	8.47	6.87	8.22
8	2,700	2.52	3.01	6.80	8.13	6.68	7.99
9	31,076	2.38	2.96	74.08	92.11	76.91	91.98
10	14,628	2.59	3.26	37.89	47.63	36.20	43.30
6	2,528	2.31	2.86	5.83	7.22	6.26	7.48
Totals	*74,332*			*176.28*	*218.15*	*183.97*	*220.02*
Difference in June	[redacted]	[redacted]	[redacted]		[redacted]	–8m^3	[redacted]
Difference in July	[redacted]	[redacted]	[redacted]	[redacted]		[redacted] –2m^3	

Notes: In greenish columns are presented the estimated WV-2 water requirements for June 29th and July 9th and in brownish columns the corresponding requirements estimated by FAO for the same months. The values of [–8m^3] and [–2m^3] are the total difference in cubic metres in June and July, respectively.

5 Summary and conclusions

The present work is one the first attempts to deploy the principles of precision farming for integrated olive tree management in the agricultural Association of Messolonghi-Nafpaktia, Southwestern Greece, by combining satellite data and methods with field measurements. It is possible to monitor irrigation and nutrient requirements efficiently by merging field measurements and satellite data at specified intervals and thus develop and implement an effective site-specific management system. Satellites seem to constitute part of an integral operational procedure due to their global repetitive coverage over an AoI, as well as their spatial and spectral resolution. The comparison of satellite data and FAO reference values has indicated that the utilisation of the very high spatial and spectral data, such as WV-2, is certainly a useful tool for farm-based stakeholders, allowing not only the extraction of trees (Karantzalos and Argialas, 2004), but also the derivation of useful parameters, such as the $K_{c(satellite)}$ and $ET_{c(satellite)}$, that can be used in the estimation of crop water and fertilisation needs. The $K_{c(satellite)}$ and $ET_{c(satellite)}$ depict better the phenological cycle of the crop and they are more close to what is 'happening in the field' and also to weather conditions, and always reflect the agricultural practises, e.g., irrigation and fertilisation, as these actions are very dynamic and modified according to crop and weather, farmer behaviour and policies (AGRO 2). The overall water requirements extracted by satellite data are less than the ones estimated by FAO method, resulting to true water-use savings and possible optimisation of the inputs, while preserving and protecting the environment. One cubic metre per hectare saving in an area of 2,552 hectares in a month is a considerable number to shape pricing policies in the direction of sustainability of irrigation services. Hence, the general rule of 120–150 m^3 per 0.1 hectare per year for the irrigation of ten-year old olive groves can be fine-tuned and be more accurate with the use of satellite data resulting to a true water saving. The half metre class spatial resolution along with eight-band narrowed spectral capability constitutes a key component in precision agriculture, where the scale and crop reparability are significant issues at field level (Spyropoulos, 2002). High spectral and spatial resolution satellites, such as WorldView-2/3/4 can be used in an operational mode for crop/tree area extraction and estimation of vegetation coefficients, such as K_c and evapotranspiration, according to its variable phenological stage, even within individual trees in small agricultural farms typical to fragmented land-use of the Mediterranean rural areas. FPAR may be systematically observed over time and it can create the geospatial intelligence knowledge correlated with N update and crop production. Farmers can look archived FPAR data distribution for the same parcel, then can estimate the *N* update and thus be more accurate in quantifying and 'quality-fying' their crop production (Dalezios et al., 2019). Olive tree farmers responded positively on the image sharpness and clarity of WV-2 satellite data. In that respect and prior to any Integrated Management Programme System compliant with AGRO 2.1 and 2.2 standards for agricultural production, farmers may consult the methodology proposed to monitor quantitatively the necessary water and fertilisation needs for their crops. The present work is expected be the basis for future work, which will provide a broad range of results and is expected to show how the farmers can optimise the water and *N* fertilisation inflows into their olive tree farms.

References

Allen, R.G., Pereira, L.S., Raes, D. and Smith, M. (1998) *Crop Evapotranspiration: Guidelines for Computing Crop Water Requirements*, Irrigation and Drainage Paper 56, 300pp., United Nations Food and Agriculture Organization, Rome, Italy.

Asrar, G., Fuch, M., Kanemasu, E.T. and Hatfield, J.L. (1984) 'Estimating absorbed photosynthetic radiation and leaf area index from spectral reflectance in wheat', *Agronomy Journal*, Vol. 76, No. 2, pp.300–306.

Bannari, A., Asalhi, H. and Teillet, P. (2002) 'Transformed difference vegetation index (TDVI) for vegetation cover mapping', *in IGARSS '02, IEE International: Proceedings of the Geoscience and Remote Sensing Symposium*, Vol. 5.

Calera, A., Campos, I., Osann, A., D'Urso, G. and Menenti, M. (2017) 'Remote sensing for crop water management: from ET modelling to services for the end users', *Sensors*, Vol. 17, No. 5 [online] https://doi.org/10.3390/s17051104.

Colombo, R., Bellingeri, D., Fasolini, D. and Marino, M.C. (2003) 'Retrieval of leaf area index in different vegetation types using high-resolution satellite data', *Remote Sensing of Environment*, Vol. 86, No. 1, pp.120–131, DOI: 10.1016/S0034-4257(03)00094-4.

Dalezios, R.N., Dercas, N., Spyropoulos, V.N. and Psomiadis, M. (2019) 'Remotely sensed methodologies for water availability and requirements in precision farming of vulnerable agriculture', *Water Resources Management*, Vol. 33, No. 4, pp.1499–1519.

Dalezios, R.N., Dercas, N., Spyropoulos, V.N. and Psomiadis, M. (2017) 'Water availability and requirements in precision farming of vulnerable agroecosystems', *European Water*, Vol. 59, No. 1, pp.387–394.

Dalezios, R.N., Spyropoulos, V.N. and Blanta, A. (2012) 'Agrometeorological remote sensing of high resolution for decision support in precision agriculture', in Helmis, C. et al. (Eds.): *Advances in Meteorology, Climatology and Atmospheric Physics, Springer Atmospheric Sciences*, pp.51–56, Springer-Verlag, Berlin, Heidelberg, DOI: 10.1007/978-3-642-29172-2_8.

Dalezios, R.N., Spyropoulos, V.N., Blanta, A. and Tarquis M.A. (2014) 'Risk identification of agricultural drought for sustainable agroecosystems', *Natural Hazards and Earth System Sciences*, special issue: 'Advances in meteorological hazards and extreme events', Vol. 14, No. 9, DOI: 10.5194/nhess-14-2435-2014.

Dercas, N., Spyropoulos, N.V., Dalezios, N.R., Psomiadis, E., Stefopoulou, A., Madonanakis, G. and Tserlikakis, N. (2017) 'Cotton evapotranspiration using very high spatial resolution WV-2 satellite data and ground measurements for precision agriculture', *WIT Transactions on Ecology and the Environment*, Vol. 220, No. 1, pp.101–107, Water Resources Management, WIT Press [online] https://doi.org/10.2495/WRM170101.

Fensholt, R., Sandholt, I. and Rasmussen, S.M. (2004) 'Evaluation of MODIS LAI, fAPAR and the relation between fAPAR and NDVI in a semi-arid environment using in situ measurements', *Remote Sensing of Environment*, Vol. 91, No. 1, pp.490–507.

Huete, A. (1988) 'A soil-adjusted vegetation index (SAVI)', *Remote Sensing of Environment*, Vol. 25, No. 3, pp.295–309.

Kanellou, C.E., Spyropoulos, V.N. and Dalezios, R.N. (2011) 'Geoinformatic intelligence methodologies for drought spatiotemporal variability in Greece', *Water Resources Management*, Vol. 25, No. 5, Springer, DOI: 10.1007/s1269-011-9948-1, ISSN: 0920-4741.

Karantzalos, G.K. and Argialas, P.D. (2004) 'Towards automatic olive tree extraction from satellite imagery', *Geo-imagery Bridging Continents, XXth ISPRS Congress*, Commission III, WG 4, HRAKLEITOS EPEAEK Research Program, European Union and the Greek Ministry of Education.

Koch, B. and Khosla, R. (2003) 'The role of precision agriculture in cropping systems', *Journal of Crop Production*, Vol. 9, Nos. 1–2, pp.361–381, DOI: 10.1300/J144v09n01_02.

Office for Official Publications of the European Communities (2006) *European Policy for Quality Agricultural Products*, EU, Directorate Agriculture, Luxembourg, ISBN: 92-79-03228-3.

Papazafeiriou, G.Z. (1999) *The Water Need of Cultivations*, Ziti Publications, Athens, ISBN: 960-431-580-3.

Spyropoulos, V.N. (1999) 'The benefits of high-resolution earth imagery in agriculture – the Ikonos system and its applications to agri-environment schemes', *1st Workshop on the Management and Monitoring of Agri-environment Schemes*, Joint Research Center (JRC), Ispra, Italy, 23–24 November.

Spyropoulos, V.N. (2002) 'Image segmentation, classification and feature extraction', *in XXII FIG International Congress. ACSM-ASPRS Conference and Technology Exhibition*, Washington, DC, 19–26 April.

Stamatiadis, S., Schepers, J.S., Evangelou, L., Tsadilas, C., Glampedakis, A., Glampedakis, M., Dercas, N., Spyropoulos, N., Dalezios, R.N. and Eskiridge, K. (2017) 'Variable-rate nitrogen fertilisation of winter wheat under high spatial resolution', *Precision Agriculture*, Vol. 19, No. 5, pp.570–587.

Updike, T. and Comp, C. (2010) *Radiometric Use of WorldView-2 Imagery*, Technical Note, DigitalGlobe, 1601 Dry Creek Drive Suite 260 Longmont, Colorado, 80503, USA.

Wiegand, L.C., Maas, J.S., Aase, K.J., Hatfield, L.J., Pinter Jr., J.P., Jackson, D.R., Kanemasu, T.E. and Lapitan, L.R. (1992) 'Multisite analyses of spectral-biophysical data for wheat', *Remote Sensing of Environment*, Vol. 42, No. 1, pp.1–21 [online] https://doi.org/10.1016/0034-4257(92)90064-Q.

Xu, O., Zhang, Y. and Li, B. (2014) 'Recent advances in pansharpening and key problems in applications', *International Journal of Image and Data Fusion*, Vol. 5, No. 3, pp.175–195 [online] https://doi.org/10.1080/19479832.2014.889227.

Yang, C., Everitt, J.H. and Bradford, J.M. (2006) 'Comparison of QuickBird satellite imagery and airborne imagery for mapping grain sorghum yield patters', *Precision Agriculture*, Vol. 7, No. 1, pp.33–44, DOI: 10.1007/ s11119-005-6788-0.

Yoder, E.R., Odhiambo, O.L. and Wright, C.W. (2005) 'Evaluation of methods for estimating daily reference crop evapotranspiration at a site in the humid southeast United States', *Applied Engineering in Agriculture*, Vol. 21, No. 2, pp.197–202, ISSN: 0883–8542.